# Fibre formation in calcium caseinate influenced by solvent isotope effect and drying method – A neutron spectroscopy study

Tian, Bei; Garcia Sakai, Victoria; Pappas, Catherine; van der Goot, Atze Jan; Bouwman, W. G.

**DOI**
10.1016/j.ces.2019.07.023

**Publication date**
2019

**Document Version**
Final published version

**Published in**
Chemical Engineering Science

**Citation (APA)**
Tian, B., Garcia Sakai, V., Pappas, C., van der Goot, A. J., & Bouwman, W. G. (2019). Fibre formation in calcium caseinate influenced by solvent isotope effect and drying method – A neutron spectroscopy study. *Chemical Engineering Science*, *207*, 1270-1277. https://doi.org/10.1016/j.ces.2019.07.023

Chemical Engineering Science 207 (2019) 1270–1277

Contents lists available at ScienceDirect

Chemical Engineering Science

journal homepage: www.elsevier.com/locate/ces

# Fibre formation in calcium caseinate influenced by solvent isotope effect and drying method – A neutron spectroscopy study

Bei Tian [a], Victoria Garcia Sakai [b], Catherine Pappas [a], Atze Jan van der Goot [c], Wim G. Bouwman [a,*]

[a] Department of Radiation Science and Technology, Faculty of Applied Science, Delft University of Technology, Mekelweg 15, 2629JB Delft, the Netherlands
[b] ISIS Neutron and Muon Facility, Science & Technology Facilities Council, Rutherford Appleton Laboratory, United Kingdom
[c] Food Process Engineering, Wageningen University, the Netherlands

## HIGHLIGHTS

- $D_2O$ affects the dynamics of calcium caseinate differently than $H_2O$.
- The effect of $D_2O$ on protein's dynamics might extend to its structuring potential.
- QENS links the molecular dynamics of calcium caseinate to its bulk fibre structure.
- A harsh and longer drying condition contributes to less active protein side groups.

## ARTICLE INFO

*Article history:*
Received 26 April 2019
Received in revised form 10 July 2019
Accepted 13 July 2019
Available online 15 July 2019

*Keywords:*
Fibre formation
Calcium caseinate
Protein dynamics
Solvent isotope effect
Drying method
Neutron spectroscopy

## ABSTRACT

We present an investigation of the dynamics of calcium caseinate as a function of hydration, solvent isotope ($H_2O$ and $D_2O$) and drying methods (roller drying and spray drying), using quasi-elastic neutron scattering (QENS). These factors are key to the formation of fibres in this material which makes it a potential candidate as a next-generation meat analogue. Using a phenomenological model, we find that the relaxation times of the dry spray dried powder decrease with increasing temperatures, while they do not change for the roller dried powder. The spectra of the hydrated samples reveal two independent picosecond processes, both reflecting localized re-orientational motions. We hypothesize that the faster motion is due to the external protein groups that are hydrophilic and the slower motion is due to the internal groups that are hydrophobic. The solvent effect of $D_2O$ is not limited to the external groups but prevails to the internal groups where less protons are mobile compared to the $H_2O$ hydrated samples. Higher temperatures narrow the number difference in mobile protons, possibly by altering the weak interactions inside the protein aggregates. These findings suggest that a harsh and longer drying process contributes to less active protein side-groups and highlight the hydrophobic effect of $D_2O$ on the fibre formation in calcium caseinate.



## 1. Introduction

The mechanism of fibre formation in calcium caseinate has been at the focus of research interest during the last decade, as these fibrous structures are promising candidates for the production of next-generation meat analogues (Manski et al., 2007; Manski et al., 2007). The fibrous calcium caseinate gel has good mechanical properties, and its structure is much more anisotropic (Wang et al., 2019) than plant-based meat analogue candidates (Dekkers et al., 2016). In view of potential applications, it is therefore important to investigate the structure and dynamics of the fibrous structure in calcium caseinate, as these studies provide valuable insight into the design of plant-based meat analogues with more pronounced anisotropic structures.

Recently, we came across an interesting observation: the calcium caseinate fibre formation is strongly influenced by the solvent isotope effect (Tian et al., 2018). 30%w/w spray dried calcium caseinate (SCaCas) mixed with $H_2O$ gives more anisotropic fibres, while roller dried calcium caseinate (RCaCas) processed under the same condition results in a homogeneous gel. When $D_2O$ is used to mix with the calcium caseinate powder, the fibres in SCaCas do not form, while RCaCas does show some fibres. Given that the only variable is the solvent, we assume that both the molecular motions of the protein and the interactions between the solvent and protein (e.g. hydrogen bonds) change because of the solvent isotope effect. To test the validity of this hypothesis,

* Corresponding author.
*E-mail address:* w.g.bouwman@tudelft.nl (W.G. Bouwman).

https://doi.org/10.1016/j.ces.2019.07.023
0009-2509/

we used quasi-elastic neutron scattering (QENS) to investigate the dynamics of both SCaCas and RCaCas on a molecular level.

QENS has been successfully applied to study the dynamics at the atomic scale of many biological systems: from globular protein such as lysozyme, myoglobin and green fluorescent protein (GFP) (Magazu et al., 2010; Roh et al., 2006; Doster et al., 1989; Nickels et al., 2012) to bio macro-molecules like tRNA, DNA and membranes (Caliskan et al., 2006; Roh et al., 2009; Chen et al., 2006; Fitter et al., 1999). The technique probes timescales and amplitudes of the dynamics and gives insights into the interactions with hydration water. The application of QENS on food materials is much less explored than on biological systems. The few existing examples focus on the hydration water dynamics. For instance, the self-diffusion constant of water in fresh bread was obtained by fitting the self-intermediate scattering function with a stretched exponential function at room temperature (Sjöström et al., 2007); A similar approach has been applied to study dehydrated fresh strawberry and rehydrated freeze-dried strawberry (Jansson et al., 2006). A study on a larger globular glycinin showed that its dynamic transition is similar to that observed in smaller proteins (Kealley et al., 2010). These investigations hint to a relation between the food matrix and the hydration water.

Until now, most of the QENS measurements were conducted on samples obtained through freeze-drying (Orecchini et al., 2002; Stadler et al., 2012; Ameseder et al., 2018), as it is assumed that this process affects less the denaturation and aggregation of the protein (Hsu et al., 2003; Claussen et al., 2007; Luck et al., 2013; Caparino et al., 2012). Though lyophilisation has its advantages, it is not used by the food industry due to its high operational costs and low throughput (Ratti, 2001). Furthermore, lyophilisation is not representative of the effect of other drying methods on the protein dynamics. As a result, investigations of the influence of spray and roller drying on the protein structure and dynamics are of great importance to the field of food science, given that these methods are commonly used for the industrial production of food biopolymers (Dehnad et al., 2016).

Our QENS investigation probes for the first time, the protein dynamics of industrially produced food powders, which can potentially mimic real meat. The experiments were performed on dry SCaCas and RCaCas powders, as well as on powders hydrated with either $D_2O$ or $H_2O$, to a hydration level of h = 0.4, which is generally considered to be a full hydration level (Gabel et al., 2002). The measurements were performed at 293 K, i.e. at room temperature, at 320 K, the temperature at which the fibres are obtained, and at 340 K where protein aggregates form reversible agglomerates.

One of the strengths of neutron scattering is the possibility to highlight, by deuteration, certain parts of the hydrogen containing samples. However, in our study, it was not possible to deuterate the caseinate. One reason is that it is an industrial product obtained from casein curd and there is a batch to batch variation. Another reason is that caseinate is composed of four sub-caseins, its structure is not well-defined and still under debate (De Kruif et al., 2012; Ingham et al., 2015). Therefore, unlike other model systems, it would have been very challenging to deuterate a specific part of the caseinate. Nevertheless, we were able to investigate the solvent isotope effect and compare the effect of hydration by using either $H_2O$ or $D_2O$. Through the data analysis we can assign the dynamics to certain protein groups and correlate them to the macroscopic observations of fibre formation.

## 2. Material and methods

### 2.1. Sample preparation

Roller and spray dried calcium caseinate powders were provided by DMV International, Veghel, The Netherlands. The solvent used throughout the drying process was $H_2O$. As their names suggest, the powders were obtained through roller drying or spray drying, which resulted in different powder morphologies. Scanning electron microscopy images were taken using JEOL JSM-IT100. The secondary electron detector was used with 1.6 kV, a probe current of 20 nA, and the magnification was 200.

For the QENS measurements, the powders were first dehydrated in a vacuum oven at 60 °C for 2 days. The dried samples were then hydrated in hydration chambers with either $D_2O$ or $H_2O$. All samples reached a hydration level of ~0.4 (weight solvent/weight dry protein powder). Approximately 400 mg of powder was loaded and sealed in an annular aluminum sample holder with a thickness of 2 mm.

The scattering cross sections of the samples were calculated according to the specifications provided by the manufacturer and are shown in Table 1. The incoherent cross section of the dry powder accounts for up to 89.6% of the signal. After hydration with $H_2O$, the scattering contribution from the protein decreased to 63.1%. After hydration with $D_2O$, assuming 20% of the hydrogen has exchanged with deuterium, the contribution of the protein to the scattering still accounts for up to 81.9%.

### 2.2. Quasi-elastic neutron scattering experiments

The QENS experiments were performed at the time-of-flight inverted geometry spectrometer IRIS (Carlile and Adams, 1992) at the ISIS neutron facility, as a function of both energy ($\omega$) and momentum transfer ($Q$). We used the [002] reflection of the pyrolytic graphite analyser, which gives an energy resolution of 17.5 μeV, and covers an energy range from −0.5 to 0.5 meV. The scattered neutrons were measured by 51 detectors that cover a $Q$-range from 0.42 to 1.85 $Å^{-1}$. During fitting of the elastic incoherent structure factor (EISF), the signals of the these 51 detectors were regrouped into 15 $Q$ values to improve statistics.

The samples were measured at 293 K, 320 K and 340 K for around 5 h, respectively. So-called elastic scans were conducted from 20 K to 340 K with an increment step of 10 K. The detector efficiency was corrected by measuring a vanadium standard. The resolution function was obtained by measuring the corresponding sample at 20 K. The data reduction was performed with the Mantid

**Table 1**
Incoherent, coherent and absolute scattering cross sections ($\sigma$) of the dry and hydrated samples calculated based on the amino acid compositions of calcium caseinate provided by the supplier.

| | Dry powder | Hydrated with 0.4 g/$H_2O$ g | | Hydrated with 0.4 g/$D_2O$ g | |
|---|---|---|---|---|---|
| | | Protein | Solvent | Protein* | Solvent |
| $\sigma_{inc}$% | 89.6 | 63.1 | 27.8 | 81.9 | 1.2 |
| $\sigma_{coh}$% | 8.0 | 5.6 | 1.3 | 10.1 | 4.4 |
| $\sigma_{abs}$% | 2.4 | 1.7 | 0.4 | 2.4 | 0 |

* Assuming 20% of the H exchanged with D.

software (Arnold et al., 2014), and the reduced spectra were analyzed using the software DAVE (Azuah et al., 2009).

## 3. Results

### 3.1. Quasi-elastic widths and amplitudes

After initial fitting, we found that two uncoupled Lorentzian functions are needed to describe the quasi-elastic contribution. For a detailed documentation of the fits, the reader is referred to the supplementary information. Our initial results also show that the full width half maximum (FWHM) $\Gamma$ of the two Lorentzian functions are $Q$-independent (supplementary information), suggesting that we observe either re-orientational or localised motions. In order to obtain accurate values of $\Gamma$, we summed the intensity of all detectors and fitted the data with the scattering function

$$S(\omega) = [A_0 \cdot \delta(\omega) + A_{\text{slow}} \cdot L_{\text{slow}}(\omega) + A_{\text{fast}} \cdot L_{\text{fast}}(\omega) + a\omega + b] \otimes R(\omega), \quad (1)$$

where $A_0 \cdot \delta(\omega)$ is the elastic scattering contribution with $A_0$ the elastic amplitude and $\delta(\omega)$ the Dirac delta function. $A_{\text{slow}}$ and $A_{\text{fast}}$ are the quasi-elastic amplitudes, $L_{\text{slow}}(\omega)$ and $L_{\text{fast}}(\omega)$ are the Lorentzian functions, and $R(\omega)$ is the resolution function. Any inelastic contributions that are outside the energy window of the instrument are accounted for by the linear background $a\omega + b$.

Fig. 1 shows the spectra measured for the SCaCas sample hydrated with $H_2O$ at three temperatures. The fits for the other samples can be found in the supplementary information, and the fitted parameters are summarised in Table 2.

The FWHM of the Lorentzian function is inversely proportional to the relaxation times. The FWHMs of the dry SCaCas powder, shown Table 2, are systematically smaller than those of the RCaCas at room temperature. While both $\Gamma_{\text{slow}}$ and $\Gamma_{\text{fast}}$ of SCaCas increase with temperature, they remain constant in RCaCas, implying that the dynamics of the protein groups in RCaCas are insensitive to temperature. The drying history that the powder has experienced is probably responsible for these differences.

Hydration increases significantly the quasi-elastic amplitudes. This is not surprising since the solvent increases the protein to be more flexible and mobile. Similar results were also obtained by for example Orecchini et al., who studied the (non) exchangeable hydrogen classes in $\beta$-lactoglobulin (Orecchini et al., 2002), and found that the quasi-elastic intensity of both the protein surface and the core groups increased with increasing hydration level.

On the other hand, hydration has little impact on the width of the Lorentzians. Unlike the dry powders, the FHWMs of all hydrated samples display a similar trend. Both $\Gamma_{\text{slow}}$ and $\Gamma_{\text{fast}}$ increase with temperature, and the corresponding relaxation times decrease from approximately 52 ps to 40 ps for the slow motion, and from 7 ps to 5.4 ps for the fast motion. The $\Gamma_{\text{slow}}$ and $\Gamma_{\text{fast}}$ reported here are in line with the values reported for other protein systems, such as the internal motion of *E.coli* (Jasnin et al., 2008) and lysozyme (Roh et al., 2006) for $\Gamma_{\text{slow}}$; Neocarzinostatin, a small all $\beta$ protein (Russo et al., 2002), Ribonuclease A (Wood et al., 2008) and the hydrophobic side-chains of native $\alpha$-lactalbumin (Bu et al., 2001) for $\Gamma_{\text{fast}}$.

Though the FWHMs of the Lorentzians follow quite similar trends for the different samples and solvents, this is not the case for their area fractions, which vary depending on the drying method and the solvent. When hydrated with $D_2O$, the $L_{\text{fast}}$ and $L_{\text{slow}}$ are slightly smaller for SCaCas than for RCaCas, which suggests that there are less mobile protons in SCaCas. On the other hand, when hydrated with $H_2O$, $L_{\text{fast}}$ and $L_{\text{slow}}$ are larger for SCaCas than for RCaCas. As far as the solvent isotope effect is concerned, $H_2O$ hydrated samples have in general higher quasi-elastic amplitudes than the $D_2O$ hydrated ones. This is most likely due to the $H_2O$ molecules that are bound to the protein surface and have dynamics that are similar to the protein. In particular, the increase of area fractions is larger for SCaCas than for RCaCas when switching from $D_2O$ to $H_2O$. These results indicate that the response of the protein dynamics to the solvent isotope effect is influenced by the drying history. A possible explanation is that the protein side-group activities are different due to either chemical reactions during processing, or to a different structural arrangement of the caseinate.

### 3.2. Elastic incoherent structure factor (EISF)

The elastic incoherent structure factor (EISF), which in essence is the area fraction of the delta function EISF = $A_0/(A_0 + A_{\text{slow}} + A_{\text{fast}})$, provides complementary information to the area fraction of the Lorentzians. We can extract quantitative information on the geometry of the atomic motion by fitting the $Q$-dependence of the EISF. For this purpose, we introduce the simple modified 'free diffusion in a sphere' model (Volino and Dianoux, 1980).

$$\text{EISF} = p + (1-p)A$$

$$\text{With } A = \int_0^\infty A_{sph} \cdot f(R,\sigma)\,dR$$

$$f(R,\sigma) = \frac{2}{\sqrt{2\pi\sigma^2}} \cdot e^{-\frac{R^2}{2\sigma^2}}, \quad (2)$$

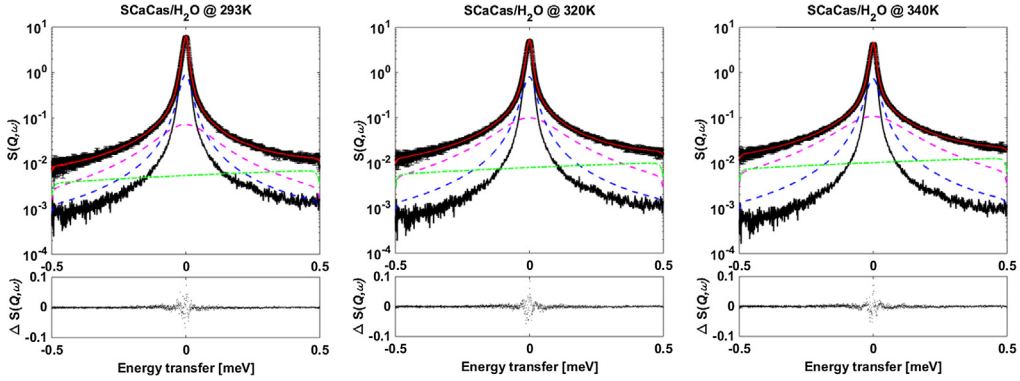


**Fig. 1.** From left to right: QENS spectra of SCaCas powder hydrated with $H_2O$ measured at 293 K, 320 K and 340 K. The residuals are plotted underneath, they are calculated as the difference between the measured and fitted S(Q, $\omega$). The delta function is represented by the black dots, the two Lorentzians are dashed lines in blue and magenta, the background is dash-dot line in green, and the total fitted curve is represented by the red line. (For interpretation of the references to colour in this figure legend, the reader is referred to the web version of this article.)

**Table 2**
Fitted parameters of SCaCas and RCaCas powders dry, hydrated with either $D_2O$ or $H_2O$ at 293 K, 320 K and 340 K. Columns 3–6 give the area fraction of the delta function, the background (bkdg) and the two Lorentzian functions ($L_{fast}$&$L_{slow}$). The area fraction is calculated as the amplitude of one component divided by the sum of all the amplitudes ($A_0 + A_{slow} + A_{fast}$ + background), the estimated error bar of the area fraction is within 1% in all cases; columns 7–8 are the corresponding FWHMs of the Lorentzian functions.

| | | Area (%) | | | FWHM (μeV) | | |
|---|---|---|---|---|---|---|---|
| | | delta | bkgd | $L_{slow}$ | $L_{fast}$ | $\Gamma_{slow}$ | $\Gamma_{fast}$ |
| SCaCas/dry | 293 K | 89.8 | 0.8 | 6.6 | 2.9 | $25 \pm 4$ | $163 \pm 17$ |
| | 320 K | 89.2 | 0.8 | 7.2 | 2.8 | $39 \pm 3$ | $239 \pm 26$ |
| | 340 K | 86.9 | 1.2 | 7.9 | 4.0 | $53 \pm 7$ | $293 \pm 79$ |
| RCaCas/dry | 293 K | 89.2 | 1.2 | 7.5 | 2.1 | $32 \pm 2$ | $247 \pm 24$ |
| | 320 K | 87.7 | 1.5 | 7.5 | 3.0 | $34 \pm 2$ | $227 \pm 18$ |
| | 340 K | 86.4 | 1.7 | 7.9 | 4.0 | $36 \pm 2$ | $226 \pm 15$ |
| SCaCas/$D_2O$ | 293 K | 74.9 | 1.9 | 16.8 | 6.4 | $26 \pm 1$ | $188 \pm 8$ |
| | 320 K | 68.1 | 2.9 | 19.2 | 9.8 | $33 \pm 1$ | $214 \pm 8$ |
| | 340 K | 63.0 | 3.3 | 21.1 | 12.6 | $36 \pm 2$ | $244 \pm 14$ |
| RCaCas/$D_2O$ | 293 K | 73.5 | 1.9 | 17.8 | 6.7 | $25 \pm 1$ | $201 \pm 77$ |
| | 320 K | 66.1 | 3.0 | 19.9 | 11.0 | $28 \pm 1$ | $202 \pm 56$ |
| | 340 K | 60.0 | 3.9 | 21.4 | 14.7 | $30 \pm 1$ | $221 \pm 67$ |
| SCaCas/$H_2O$ | 293 K | 61.0 | 2.6 | 25.6 | 10.9 | $26 \pm 1$ | $196 \pm 5$ |
| | 320 K | 52.1 | 4.0 | 26.2 | 17.7 | $31 \pm 1$ | $219 \pm 4$ |
| | 340 K | 46.5 | 5.4 | 26.3 | 21.9 | $33 \pm 1$ | $240 \pm 4$ |
| RCaCas/$H_2O$ | 293 K | 65.5 | 2.4 | 22.4 | 9.6 | $25 \pm 1$ | $182 \pm 6$ |
| | 320 K | 57.6 | 3.7 | 23.9 | 14.8 | $32 \pm 1$ | $216 \pm 5$ |
| | 340 K | 52.8 | 4.4 | 24.3 | 18.5 | $33 \pm 2$ | $235 \pm 9$ |

where $p$ is the population of immobile protons and $A_{sph} = [\frac{3j_1(QR)}{QR}]^2$, with $j_1$ the first-order Bessel function of the first kind. The Gaussian distribution $f(R, \sigma)$ accounts for the heterogeneity of the samples (Russo et al., 2002) with $\sigma$ the variance. The average diffusion radius of the sphere is $R_0 = \sigma\sqrt{\frac{2}{\pi}}$.

Fig. 2 shows the experimental results and the excellent fits to the data. The deduced parameters are given in Table 3. The population of the immobile protons $p$ of all samples decreases as temperature increases. This trend is also consistent with the area fractions of the quasi-elastic amplitudes, which increase with increasing temperature. Interestingly, at 293 K, SCaCas hydrated with $H_2O$ has significantly less immobile protons than the other samples. However, the difference between this sample and the rest reduces as temperature increases. This indicates that SCaCas hydrated with $H_2O$ is the sample with the most mobile protons whereas high temperatures mitigate the solvent effect.

The diffusion radius $R_0$ is about 1.9 Å for the $D_2O$ hydrated samples, and 3.0 Å for the $H_2O$ hydrated ones. Both radii are much larger than the reported value of 1 Å for the methyl-group rotation

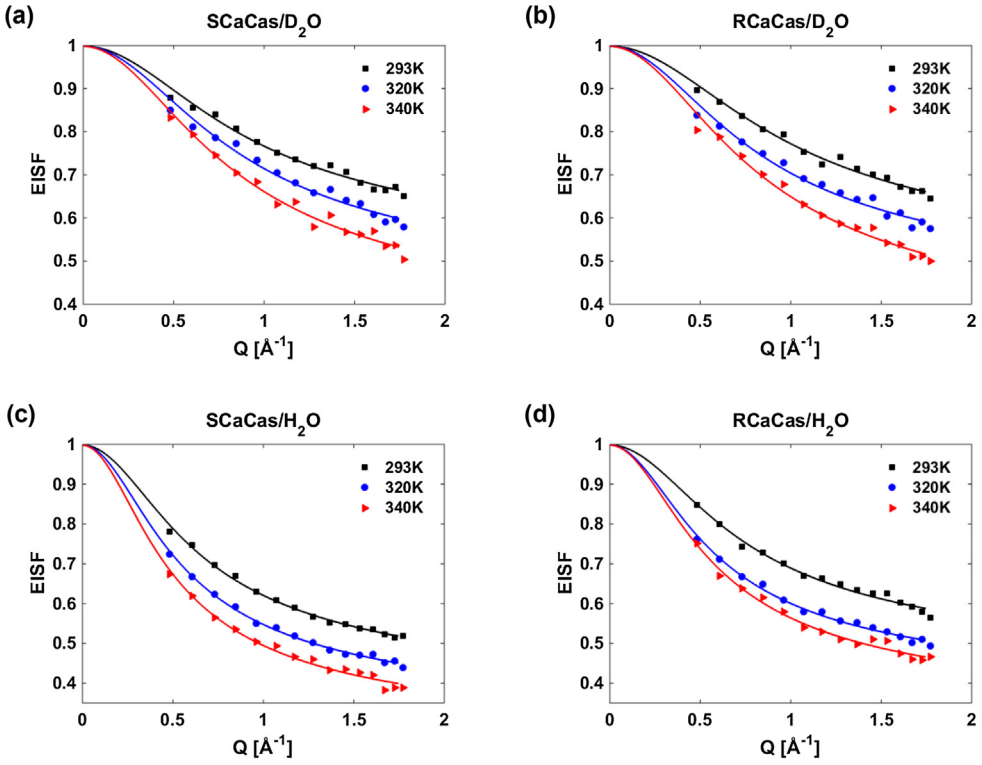


**Fig. 2.** EISF fitted with the free diffusion in a sphere model, plotted as a function of $Q$ at different temperatures. SCaCas and RCaCas powders are hydrated with $D_2O$ (a and b) or $H_2O$ (c and d).

**Table 3**
Fitted values of $p$ and $R_0$ of SCaCas and RCaCas hydrated with either $D_2O$ or $H_2O$ at 293 K, 320 K and 340 K.

| | Temperature | SCaCas/$D_2O$ | RCaCas/$D_2O$ | SCaCas/$H_2O$ | RCaCas/$H_2O$ |
|---|---|---|---|---|---|
| $p$ | 293 K | 0.49 ± 0.04 | 0.46 ± 0.04 | 0.36 ± 0.02 | 0.43 ± 0.03 |
| | 320 K | 0.40 ± 0.05 | 0.41 ± 0.04 | 0.31 ± 0.01 | 0.37 ± 0.02 |
| | 340 K | 0.32 ± 0.05 | 0.30 ± 0.04 | 0.26 ± 0.02 | 0.32 ± 0.02 |
| $R_0$ (Å) | 293 K | 1.8 ± 0.2 | 1.7 ± 0.2 | 2.7 ± 0.1 | 2.3 ± 0.2 |
| | 320 K | 2.0 ± 0.2 | 2.1 ± 0.2 | 3.2 ± 0.1 | 3.0 ± 0.2 |
| | 340 K | 2.1 ± 0.2 | 2.1 ± 0.2 | 3.6 ± 0.3 | 3.1 ± 0.2 |

(Frick and Fetters, 1994). Thus, these radii probably implicate the hydrophilic side chains or the flexible regions of the protein that are participating in the motions. The radii of the $D_2O$ hydrated samples are close to those of folded globular proteins such as lysozyme, myoglobin or GFP (Pérez et al., 1999; Roh et al., 2006; Nickels et al., 2012). For the $H_2O$ hydrated samples, the radii are similar to those of $\beta$-casein, tRNA and *E.coli* (Dhindsa et al., 2014; Perticaroli et al., 2014; Roh et al., 2009; Jasnin et al., 2008).

The difference in the diffusion radii of $H_2O$ and $D_2O$ hydrated samples may be due to either the different incoherent cross sections of hydrogen and deuterium, or to the solvent effect. On the basis of our observations, we are inclined to attribute this effect to the latter. The reason is that the diffusion radius reflects the dynamics of the side chains rather than the dynamics of the H atoms. Given that the molecular mass of side chains is not affected substantially by deuteration, the difference in the diffusion radius must be attributed to the solvent effect. Furthermore, since proteins with open structures such as caseinate tend to have larger diffusion radii than proteins with well-defined folded structures, the fact that the radii of the $D_2O$ hydrated samples are smaller than those of the $H_2O$ hydrated ones indicates that a more hydrophobic environment constrains the diffusive motions of calcium caseinate.

The temperature dependence of mobile protons has been seen in many systems and has been attributed to protein denaturation or thermal unfolding (Russo et al., 2002; Gibrat et al., 2008; Dhindsa et al., 2014). Our preliminary differential scanning calorimetry data (supplementary information) show small bumps in the heat capacity of all the samples between 320 and 340 K, which indicate structural changes. We attribute this phenomenon to the relaxation of hydrogen bond networks (Doster et al., 1999) and the swelling of protein aggregates (Gibrat et al., 2008), instead of to irreversible denaturation or thermal unfolding. The reasons are twofold. One is that the diffusion radii increase with increasing temperature. This leads to larger diffusion volumes, which are likely to result from the swelling of caseinate aggregates and the breakage of hydrogen bonds at mild heating temperatures, such as below 340 K. On the other hand, when a protein with a well-defined structure undergoes an irreversible denaturation, its flexibility is constrained and its diffusion radius usually decreases (Russo et al., 2002; Dhindsa et al., 2014). Consequently, the diffusion volume for the side-chains is reduced as well.

The other reason is related to the water content of the samples. Compared to dry powders, thermal unfolding is observed more often in solutions, since more solvents decrease the protein stability. On the one hand, the protein's freedom of movement is limited by the low water content (Anandharamakrishnan et al., 2007); on the other hand, more energy is needed to mobilize the first or second hydration layer, as these water molecules are tightly bound to the protein surface (Colombo et al., 2010). Given the low water content of our samples (0.4 g solvent/g dry powder), the temperature that would trigger irreversible denaturation is most likely higher than 340 K.

### 3.3. Elastic window scan

In order to follow the temperature dependence of the dynamics at the molecular scale, we performed elastic window scans up to temperatures above physiological conditions. From the measurements, we deduced both the elastic incoherent intensity $\Delta I_{el}$ and the mean-square atomic displacement (MSD) $\langle u^2 \rangle$. $\Delta I_{el}$ is calculated as the difference between the normalized elastic intensity of the hydrated and the dry samples: $\Delta I_{el} = \frac{I_{\text{hydrated}}(T)}{I_{\text{hydrated}}(20K)} - \frac{I_{\text{dry}}(T)}{I_{\text{dry}}(20K)}$. The MSD is obtained by fitting the elastic incoherent intensity using the Gaussian approximation: $\langle u^2 \rangle = -\frac{3}{Q^2} \ln[\frac{I_{el}(Q,T)}{I_{el}(Q,20K)}]$. $\Delta I_{el}$ is summed over all the $Q$'s while the MSD is obtained from the Q-dependent $I_{el}$. Both parameters provide qualitative, complementary information of the dynamics of the samples.

The temperature dependence of $\Delta I_{el}$ is shown in Fig. 3(a). All samples display a sharp decrease of $\Delta I_{el}$ at around 250 K, which corresponds to the onset of protein anharmonic motions enabled by the presence of solvent (Gabel et al., 2002; Doster et al., 1999). Below 250 K, the decrease of $\Delta I_{el}$ for the $H_2O$ hydrated SCaCas is slightly more gradual than the others and starts at lower temperatures. Only RCaCas hydrated with $H_2O$ shows an elastic intensity higher than the dry sample, which is consistent with

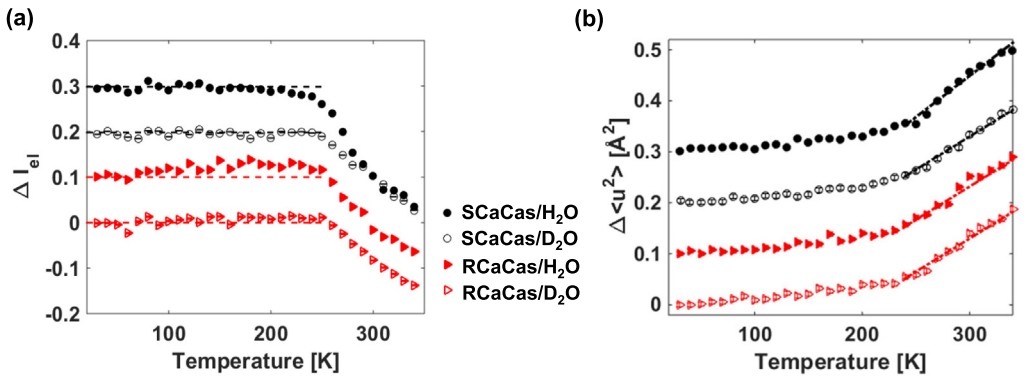


**Fig. 3.** (a) Change of the elastic incoherent intensity $\Delta I_{el}$ as a function of temperature. (b) MSDs of the hydrated samples as a function of temperature. For clarity, the plots of RCaCas hydrated with $H_2O$ (filled triangle), SCaCas hydrated with $D_2O$ (hollow circle) and $H_2O$ (filled circle) are shifted by 0.1, 0.2 and 0.3, respectively. The dashed lines are guides to the eye.

the assumption that hydration increases the stiffness of the protein structure at low temperatures (Nickels et al., 2012; Wood et al., 2008). Above 250 K, the slope of $\langle u^2 \rangle$ vs. temperature shown in Fig. 3(b) provides an empirical indication of the protein flexibility and resilience, as suggested by Zaccai (2000, 2011). According to this work, the steeper the slope, the more flexible the protein structure, which implies that more conformational changes are possible. SCaCas hydrated with $H_2O$ has a slightly steeper slope than the other samples, suggesting that it should be more prone to alignment under shear.

## 4. Discussion

This study has been initiated by the experimental observation that the isotope effect of solvent alters the fibre formation in calcium caseinate. The QENS investigation presented above reveals systematic differences at the microscopic scale. To connect the macroscopic findings with the microscopic results, we will discuss below some important aspects.

(1) Hydration scenario of the calcium caseinate powder.
It is generally agreed that the four sub-caseins in caseinate (Fig. 4(a)) (Horne, 2002) self-assemble into an open, micelle-like structure in solution (Fig. 4(b)) (Holt, 1992). Different drying methods used to obtain the protein powder cause the micelle-like structure to collapse into compact aggregates (Fig. 4(c)). This suggests that little space is available for diffusive motions, which is in line with the FWHMs of the Lorentzians that point to only re-orientational, localized motions. Moreover, though the micelle-like structure is regarded as 'open', it is unlikely that water molecules diffuse freely into the hydrophobic core during hydration of the powder (Fig. 4(d)). Based on these structural considerations, we discuss two possible explanations for the quasi-elastic amplitudes. One is that the fast and slow Lorentzians correspond to the small and large protein side-groups respectively. However, if this would have been the case, one would expect the trend in the area fraction with temperature to be the same for different solvents. This is not in line with the experimental results, as the $L_{slow}$ of $H_2O$ hydrated samples remains unchanged with increasing temperature while it increases for $D_2O$. The other possible explanation is that the fast Lorentzian represents the motions of protein groups that are exposed to the solvent (i.e. hydrophilic groups) and that the slow Lorentzian represents the groups that are not accessible to the solvent (i.e. hydrophobic groups). This explanation is in line with the experimental observations, as the area fraction of $L_{slow}$ is much higher than that of $L_{fast}$, reflecting the fact that there are more hydrophobic sub-caseins ($\alpha_{s1,s2}$- &$\beta$-casein) than hydrophilic sub-caseins ($\kappa$-casein). In the following, we will adopt this assumption and consider that the fast and slow Lorentzians represent the hydrophilic and hydrophobic side-groups of caseinate respectively.

(2) Representativeness of the measured hydration level.
A hydration level of h = 0.4 is generally regarded as sufficient to have the protein surface completely covered by at least 1 layer of water molecules (Gabel et al., 2002). This first hydration layer is considered to be bound or non-freezable (Kinsella, 1982). In the actual production of the fibrous material, a higher hydration level of h = 2.3 is used. Thus, it might be questionable whether the protein dynamics at h = 0.4 is representative of the dynamics at higher hydration levels. In this respect we note that one caseinate aggregate is larger than a globular protein and thus has a lower surface to volume ratio. Therefore, in that case, h = 0.4 would lead to more than 1 layer of hydration water. This is also confirmed experimentally, as we observe Bragg peaks from crystalline $D_2O$ at 20 K, using the additional diffraction detector from IRIS (supplementary information). Furthermore, the water activity of milk protein powder follows a sigmoidal increase with hydration content (Haque and Roos, 2004; Ostrowska-

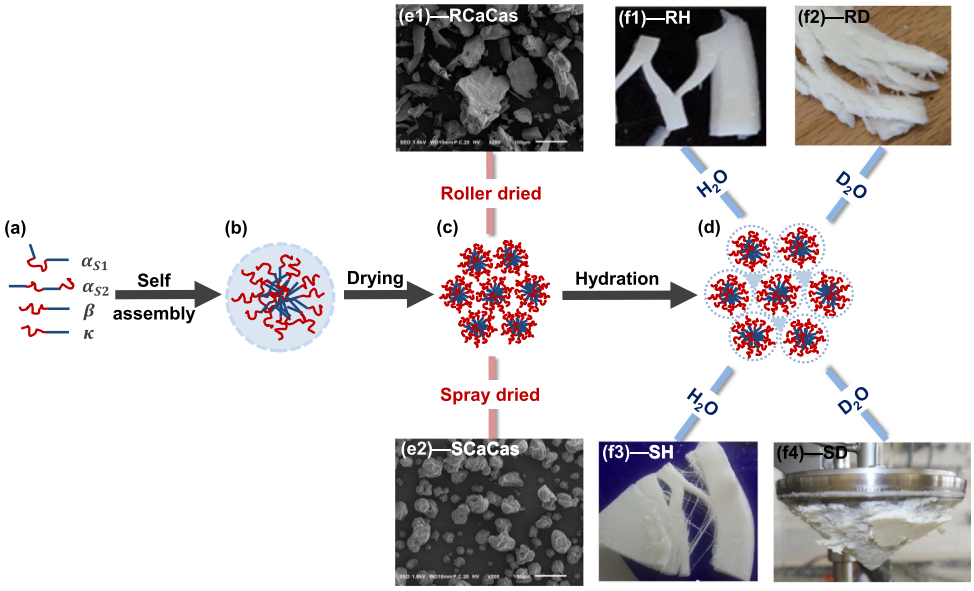


**Fig. 4.** Schematic illustration of the status of the calcium caseiante aggregates from solution (a&b) to dried powders (c&e) and to re-hydration with different solvents (d&f). (a) The four sub-caseins are depicted according to the Horne (2003), where the straight lines represent the hydrophobic region and the twisting lines represent the hydrophilic region. (b) A simplified depiction of one micelle-like aggregate in solution before drying, based on the model from the De Kruif et al. (2012). Note, $Ca^{2+}$ ions distribute homogeneously inside the aggregates, but are not shown in the drawing since they are not the interest of this discussion. (c) After drying, the micelle-like aggregates collapse into bigger aggregates that form the powder particle. (d) After hydration, each individual aggregate is surrounded by a thin layer of solvent (blue dashed lines), with some free solvent dispersed in between (blue triangle). (e) Scanning electron microscopy images of dried RCaCas (e1) and SCaCas (e2) powders. (f1-2): pictures of RCaCas gels made with $H_2O$ and $D_2O$; (f3–4): pictures of SCaCas gels made with $H_2O$ and $D_2O$. (For interpretation of the references to colour in this figure legend, the reader is referred to the web version of this article.)

Ligeza et al., 2014). Based on the moisture sorption isotherm, the water activity of the powder exceeds 0.9 when h = 0.4, a state where water is freezable. We thus concluded that the observed dynamics at h = 0.4 are representative for the behaviour at higher hydration level.

(3) Effect of the drying history on the activity of the protein. Fig. 4(e1-2) shows a clear difference in the powder morphology of roller and spray dried calcium caseinate on the micrometer length scales. It is therefore likely that the arrangements of the sub-micelles and micelle-like aggregates are also different. This is indirectly reflected in the QENS results where the dynamics between the dry powders are different. At room temperature, SCaCas has longer relaxation times than RCaCas. The relaxation times of SCaCas shorten with increasing temperature, while they remain unchanged for RCaCas. We assume that the drying history explains these discrepancies. RCaCas went through a longer heating time and at higher temperatures during drying than SCaCas. Longer times give the protein more possibilities to re-order into a thermodynamically more favourable state. In addition, a more intensive heating process may modify the micelle arrangement and even damage certain side-groups. As a result, RCaCas has probably a different structure or less active side-groups than SCaCas, which explains why its FWHMs are less affected by temperature.

(4) Solvent isotope effect on caseinate fibre formation. The most distinct macroscopic difference lies in the appearance of the fibrous gels. The use of $H_2O$ results in intact and homogeneous gels in both RCaCas (RH) and SCaCas (SH) (Fig. 4(f1,3)); On the other hand, $D_2O$ leads to a paste with inconsistent texture and expelled water (Fig. 4(f2,4)). Poor gelation behaviour can be due to a reduced water binding capacity and/or to a strong hydrophobic interaction. This is not surprising as it is indeed assumed that $D_2O$ contributes to weaker hydrogen bonds and promotes hydrophobic interaction (Efimova et al., 2007). Our QENS results also support this assumption as $L_{slow}$ is smaller in $D_2O$ hydrated samples, suggesting that less protons are mobile in the hydrophobic cores because of the solvent. Furthermore, with increasing temperature, $L_{slow}$ increases in the $D_2O$ hydrated samples, whereas it remains constant in the $H_2O$ hydrated ones. This difference may be due to the subtle changes of weak interactions (e.g. hydrophobic interaction, hydrogen bonding, Van der Waals interactions) (De Kruif et al., 2012) inside the hydrophobic cores. Higher temperatures indeed increase the hydrophobic interaction but also facilitate the breakage of hydrogen bonds which gives rise to more mobile protons. Therefore, the counterbalance in these weak interactions may be responsible for the different behaviour of $L_{slow}$.
As a final remark, the $H_2O$ hydrated SCaCas behaves differently from the rest of the samples: it has the highest quasi-elastic amplitudes (Section 3.1), the largest population of mobile protons, the largest diffusion radius (Section 3.2), and the steepest slope of MSD above 250 K (Section 3.3). These results imply that this sample combines a higher proton mobility with a higher diffusion amplitude, which are both beneficial to protein aggregates interactions. As a more flexible structure is important for the alignment of the aggregates upon deformation, our study provides a strong link between the dynamics probed by QENS and the macroscopic fibre formation in calcium caseinate.

## 5. Conclusion

Our QENS investigation sheds light on the solvent isotope effect of $H_2O$ and $D_2O$ on two industrially obtained protein powders: roller dried (RCaCas) and spray dried (SCaCas) calcium caseinate at physiological temperatures.

We analysed the data using a phenomenological model assuming two independent dynamical processes. A first result concerns the dry powder, the behaviour of which depends very much on the drying method. The relaxation times of the dry SCaCas are longer than of the dry RCaCas at room temperature, and they shorten with increasing temperature. The higher susceptibility of SCaCas to temperature may be due to the milder drying conditions.

The results of the hydrated powders show two re-orientational, picosecond motions: a fast one $\Gamma_{fast}$ attributed to the external, hydrophilic protein groups and a slow one $\Gamma_{slow}$ representing the internal, hydrophobic and solvent non-accessible regions.

The solvent isotope effect is found mostly in the quasi-elastic amplitudes and less in the relaxation times. The $D_2O$ hydrated samples have less mobile protons at the hydrophobic cores, as $D_2O$ promotes hydrophobic interaction. The EISF results are in agreement with these findings, because samples hydrated with $D_2O$ have less mobile protons and smaller diffusion radii. Temperature mitigates the solvent isotope effect by altering the weak interactions inside the micelles. In addition, the analysis of the elastic window scan suggests that SCaCas hydrated with $H_2O$ has a lower onset temperature of the dynamic transition and a more flexible conformation than the other samples. This sample also has the most anisotropic fibres.

To summarise, with QENS we were able to distinguish the dynamics between powders dried using different methods, and we could detect the solvent isotope effect of hydrated powders. We have thus established a correlation between the differences of the protein dynamics on the microscopic level and the resulting different bulk fibre structures.

## Declaration of Competing Interest

The authors declared that there is no conflict of interest.

## Acknowledgment

Experiments at the ISIS Pulsed Neutron and Muon Source were supported by a beamtime allocation from the Science and Technology Facilities Council. This work is part of the research project SSCANFoods (project number 13386), which is partly financed by the Netherlands Organisation for Scientific Research (NWO). We would like to thank Anton Lefering for assisting with the DSC measurements and the sample hydration.

## Appendix A. Supplementary material

Supplementary data associated with this article can be found, in the online version, at https://doi.org/10.1016/j.ces.2019.07.023.

## References

Ameseder, F., Radulescu, A., Khaneft, M., Lohstroh, W., Stadler, A.M., 2018. Homogeneous and heterogeneous dynamics in native and denatured bovine serum albumin. Phys. Chem. Chem. Phys. 20 (7), 5128–5139.

Anandharamakrishnan, C., Rielly, C., Stapley, A., 2007. Effects of process variables on the denaturation of whey proteins during spray drying. Dry. Technol. 25 (5), 799–807.

Arnold, O., Bilheux, J.-C., Borreguero, J.M., Buts, A., Campbell, S.I., Chapon, L., Doucet, M., Draper, N., Leal, R.F., Gigg, M.A., et al., 2014. Mantid-Data analysis and visualization package for neutron scattering and $\mu$SR experiments. Nucl. Instrum. Meth. Phys. Res. Sect. A: Accel. Spectrom. Detect. Assoc. Equip. 764, 156–166.

Azuah, R.T., Kneller, L.R., Qiu, Y., Tregenna-Piggott, P.L.W., Brown, C.M., Copley, J.R. D., Dimeo, R.M., 2009. DAVE: a comprehensive software suite for the reduction, visualization, and analysis of low energy neutron spectroscopic data. J. Res. Natl. Inst. Stand. Technol. 114 (6), 341.

Bu, Z., Cook, J., Callaway, D.J.E., 2001. Dynamic regimes and correlated structural dynamics in native and denatured α-lactalbumin. J. Mol. Biol. 312 (4), 865–873.
Caliskan, G., Briber, R.M., Thirumalai, D., Garcia-Sakai, V., Woodson, S.A., Sokolov, A. P., 2006. Dynamic transition in tRNA is solvent induced. J. Am. Chem. Soc. 128 (1), 32–33.
Caparino, O., Tang, J., Nindo, C., Sablani, S., Powers, J., Fellman, J., 2012. Effect of drying methods on the physical properties and microstructures of mango (philippine 'carabao'var.) powder. J. Food Eng. 111 (1), 135–148.
Carlile, C.J., Adams, M.A., 1992. The design of the IRIS inelastic neutron spectrometer and improvements to its analysers. Phys. B: Condens. Matter 182 (4), 431–440.
Chen, S.H., Liu, L., Chu, X., Zhang, Y., Fratini, E., Baglioni, P., Faraone, A., Mamontov, E., 2006. Experimental evidence of fragile-to-strong dynamic crossover in DNA hydration water. J. Chem. Phys. 125, 171103.
Claussen, I., Strømmen, I., Egelandsdal, B., Strætkvern, K., 2007. Effects of drying methods on functionality of a native potato protein concentrate. Dry. Technol. 25 (6), 1091–1098.
Colombo, A., Ribotta, P.D., LEOn, A.E., 2010. Differential scanning calorimetry (dsc) studies on the thermal properties of peanut proteins. J. Agric. Food Chem. 58 (7), 4434–4439.
Dehnad, D., Jafari, S.M., Afrasiabi, M., 2016. Influence of drying on functional properties of food biopolymers: from traditional to novel dehydration techniques. Trends Food Sci. Technol. 57, 116–131.
Dekkers, B.L., Nikiforidis, C.V., van der Goot, A.J., 2016. Shear-induced fibrous structure formation from a pectin/SPI blend. Innov. Food Sci. Emerg. Technol. 36, 193–200.
De Kruif, C.G., Huppertz, T., Urban, V.S., Petukhov, A.V., 2012. Casein micelles and their internal structure. Adv. Colloid Interf. Sci. 171, 36–52.
Dhindsa, G.K., Tyagi, M., Chu, X.-Q., 2014. Temperature-dependent dynamics of dry and hydrated β-casein studied by quasielastic neutron scattering. J. Phys. Chem. B 118 (37), 10821–10829.
Doster, W., Settles, M., et al., 1999. The dynamical transition in proteins: the role of hydrogen bonds. Nato ASI Ser. A Life Sci. 305, 177–194.
Doster, W., Cusack, S., Petry, W., 1989. Dynamical transition of myoglobin revealed by inelastic neutron scattering. Nature 337 (6209), 754.
Efimova, Y.M., Haemers, S., Wierczinski, B., Norde, W., Van Well, A.A., 2007. Stability of globular proteins in $H_2O$ and $D_2O$. Biopolymers 85 (3), 264–273.
Fitter, J., Lechner, R.E., Dencher, N.A., 1999. Interactions of hydration water and biological membranes studied by neutron scattering. J. Phys. Chem. B 103 (38), 8036–8050.
Frick, B., Fetters, L.J., 1994. Methyl group dynamics in glassy polyisoprene: a neutron backscattering investigation. Macromolecules 27 (4), 974–980.
Gabel, F., Bicout, D., Lehnert, U., Tehei, M., Weik, M., Zaccai, G., 2002. Protein dynamics studied by neutron scattering. Quart. Rev. Biophys. 35 (4), 327–367.
Gibrat, G., Assairi, F.L., Blouquit, Y., Craescu, C.T., Bellissent-Funel, M.-C., 2008. Biophysical study of thermal denaturation of apo-calmodulin: dynamics of native and unfolded states. Biophys. J. 95 (11), 5247–5256.
Haque, M.K., Roos, Y.H., 2004. Water sorption and plasticization behavior of spray-dried lactose/protein mixtures. J. Food Sci. 69 (8), E384–E391.
Holt, C., 1992. Structure and stability of bovine casein micelles. Adv. Protein Chem. 43, 63–151.
Horne, D.S., 2002. Casein structure, self-assembly and gelation. Curr. Opin. Colloid Interface Sci. 7 (5–6), 456–461.
Horne, D.S., 2003. Casein micelles as hard spheres: limitations of the model in acidified gel formation. Colloids Surf. A: Physicochem. Eng. Aspects 213 (2–3), 255–263.
Hsu, C.-L., Chen, W., Weng, Y.-M., Tseng, C.-Y., 2003. Chemical composition, physical properties, and antioxidant activities of yam flours as affected by different drying methods. Food Chem. 83 (1), 85–92.
Ingham, B., Erlangga, G.D., Smialowska, A., Kirby, N.M., Wang, C., Matia-Merino, L., Haverkamp, R.G., Carr, A.J., 2015. Solving the mystery of the internal structure of casein micelles. Soft Matter 11 (14), 2723–2725.
Jansson, H., Howells, W.S., Swenson, J., 2006. Dynamics of fresh and freeze-dried strawberry and red onion by quasielastic neutron scattering. J. Phys. Chem. B 110 (28), 13786–13792.
Jasnin, M., Moulin, M., Haertlein, M., Zaccai, G., Tehei, M., 2008. In vivo measurement of internal and global macromolecular motions in Escherichia coli. Biophys. J. 95 (2), 857–864.
Kealley, C.S., Sokolova, A.V., Kearley, G.J., Kemner, E., Russina, M., Faraone, A., Hamilton, W.A., Gilbert, E.P., 2010. Dynamical transition in a large globular protein: macroscopic properties and glass transition. Biochim. Biophys. Acta (BBA)-Proteins Proteom. 1804 (1), 34–40.
Kinsella, J., 1982. Relationships between structure and functional properties of food proteins. Food Proteins 1, 51–103.
Luck, P., Vardhanabhuti, B., Yong, Y., Laundon, T., Barbano, D., Foegeding, E., 2013. Comparison of functional properties of 34% and 80% whey protein and milk serum protein concentrates. J. Dairy Sci. 96 (9), 5522–5531.
Magazu, S., Migliardo, F., Benedetto, A., 2010. Mean square displacements from elastic incoherent neutron scattering evaluated by spectrometers working with different energy resolution on dry and hydrated ($H_2O$ and $D_2O$) lysozyme. J. Phys. Chem. B 114 (28), 9268–9274.
Manski, J.M., van der Goot, A.J., Boom, R.M., 2007. Advances in structure formation of anisotropic protein-rich foods through novel processing concepts. Trends Food Sci. Technol. 18 (11), 546–557.
Manski, J.M., van der Goot, A.J., Boom, R.M., 2007. Formation of fibrous materials from dense calcium caseinate dispersions. Biomacromolecules 8 (4), 1271–1279.
Nickels, J.D., O'Neill, H., Hong, L., Tyagi, M., Ehlers, G., Weiss, K.L., Zhang, Q., Yi, Z., Mamontov, E., Smith, J.C., et al., 2012. Dynamics of protein and its hydration water: neutron scattering studies on fully deuterated GFP. Biophys. J. 103 (7), 1566–1575.
Orecchini, A., Paciaroni, A., Bizzarri, A.R., Cannistraro, S., 2002. Dynamics of different hydrogen classes in β-lactoglobulin: a quasielastic neutron scattering investigation. J. Phys. Chem. B 106 (29), 7348–7354.
Ostrowska-Ligeza, E., Jakubczyk, E., Górska, A., Wirkowska, M., Bryś, J., 2014. The use of moisture sorption isotherms and glass transition temperature to assess the stability of powdered baby formulas. J. Therm. Anal. Calorim. 118 (2), 911–918.
Pérez, J., Zanotti, J.-M., Durand, D., 1999. Evolution of the internal dynamics of two globular proteins from dry powder to solution. Biophys. J. 77 (1), 454–469.
Perticaroli, S., Nickels, J.D., Ehlers, G., Mamontov, E., Sokolov, A.P., 2014. Dynamics and rigidity in an intrinsically disordered protein, β-casein. J. Phys. Chem. B 118 (26), 7317–7326.
Ratti, C., 2001. Hot air and freeze-drying of high-value foods: a review. J. Food Eng. 49 (4), 311–319.
Roh, J.H., Curtis, J.E., Azzam, S., Novikov, V.N., Peral, I., Chowdhuri, Z., Gregory, R.B., Sokolov, A.P., 2006. Influence of hydration on the dynamics of lysozyme. Biophys. J. 91 (7), 2573–2588.
Roh, J.H., Briber, R.M., Damjanovic, A., Thirumalai, D., Woodson, S.A., Sokolov, A.P., 2009. Dynamics of tRNA at different levels of hydration. Biophys. J. 96 (7), 2755–2762.
Russo, D., Pérez, J., Zanotti, J.-M., Desmadril, M., Durand, D., 2002. Dynamic transition associated with the thermal denaturation of a small beta protein. Biophys. J. 83 (5), 2792–2800.
Sjöström, J., Kargl, F., Fernandez-Alonso, F., Swenson, J., 2007. The dynamics of water in hydrated white bread investigated using quasielastic neutron scattering. J. Phys.: Condens. Matter 19 (41), 415119.
Stadler, A.M., Pellegrini, E., Johnson, M., Fitter, J., Zaccai, G., 2012. Dynamics-stability relationships in apo-and holomyoglobin: a combined neutron scattering and molecular dynamics simulations study. Biophys. J. 102 (2), 351–359.
Tian, B., Wang, Z., van der Goot, A.J., Bouwman, W.G., 2018. Air bubbles in fibrous caseinate gels investigated by neutron refraction, x-ray tomography and refractive microscope. Food Hydrocol. 83, 287–295.
Volino, F., Dianoux, A.J., 1980. Neutron incoherent scattering law for diffusion in a potential of spherical symmetry: general formalism and application to diffusion inside a sphere. Mol. Phys. 41 (2), 271–279.
Wang, Z., Tian, B., Boom, R., van der Goot, A.J., 2019. Air bubbles in calcium caseinate fibrous material enhances anisotropy. Food Hydrocol. 87, 497–505.
Wood, K., Caronna, C., Fouquet, P., Haussler, W., Natali, F., Ollivier, J., Orecchini, A., Plazanet, M., Zaccai, G., 2008. A benchmark for protein dynamics: Ribonuclease a measured by neutron scattering in a large wavevector-energy transfer range. Chem. Phys. 345 (2–3), 305–314.
Zaccai, G., 2000. How soft is a protein? A protein dynamics force constant measured by neutron scattering. Science 288 (5471), 1604–1607.
Zaccai, G., 2011. Neutron scattering perspectives for protein dynamics. J. Non-Crystal. Solids 357 (2), 615–621.